Published in final edited form as:

J Neurointerv Surg. 2018 April ; 10(4): 411–415. doi:10.1136/neurintsurg-2017-013264.

Rabbit Aneurysm Models Mimic Histologic Wall Types Identified in Human Intracranial Aneurysms

Shunli Wang[1,2], **Daying Dai**[1], **Praveen Kolumam Parameswaran**[1], **Ramanathan Kadirvel**[1], **Yong-Hong Ding**[1], **Anne M. Robertson**[3], and **David F. Kallmes**[1]

[1]Applied Neuroradiology Research Laboratory, Department of Radiology, Mayo Clinic, Rochester, Minnesota

[2]Department of Pathology, Shanghai East Hospital, Tongji University, Shanghai, China

[3]Center for Biological Imaging, University of Pittsburgh, Pittsburgh, PA, USA

Abstract

Background—Semiquantitative scales correlate histopathologic findings in the walls of human aneurysms with rupture status. We applied such a scale in the rabbit elastase-induced aneurysm model to determine whether rabbit histologic types mimic the full range of histologic subtypes of humans.

Materials and Methods—Twenty-seven elastase-induced female rabbit aneurysms were studied, harvested at 2 weeks (n=5) and 12 weeks (n=22). Paraffin-embedded sections received hematoxylin-eosin and Verhoeff-Van Gieson staining. Immunohistochemistry was performed for alpha-smooth muscle actin and CD31 for endothelial cells. Scoring used a semiquantitative scale based on human aneurysm tissue, divided into 4 subtypes on the basis of cellular and extracellular matrix findings: type A, linear organized smooth muscle cell (SMC) and intact endothelium; type B, thickened wall with disorganized, proliferating SMC; type C, thick, collagenized and hypocellular wall with or without organizing thrombosis and D, extremely thin, hypocellular wall. Separate scoring was performed of aneurysm neck and proximal and distal zones.

Results—Findings compatible with all subtypes of human aneurysm tissue were identified. Types A and C were found in 13 (48%) and 11 (41%) of 27 aneurysms and in the proximal and distal wall at both time points. Type B was found in 16 aneurysms (59%), exclusively at the neck at both time points; type D, in 14 aneurysms (52%), exclusively at proximal and distal zones of 12-week aneurysms.

Corresponding author: Daying, Dai, MD, PhD, Department of Radiology, Mayo Clinic, 200 First St SW, Rochester, MN 55905, Dai.Daying@mayo.edu, 507-266-3350, 507-255-7872 (fax).

COMPETING INTERESTS STATEMENT

None

CONTRIBUTORSHIP STATEMENT

Y-HD contributed to the aneurysm model creation.

SW, DD, and PKP contributed to tissue processing, slides staining, interpretation of data, and drafting of the manuscript.

RK, AMR, and DFK contributed to the conception and design of the study and to revision of the article critically for important intellectual content.

DATA SHARING

All authors have read the manuscript and have approved the submission of the manuscript. All authors have access to the raw data.

Conclusions—Wall of elastase-induced rabbit aneurysm demonstrates histologic findings similar to the 4 categories of human cerebral aneurysms based on cellular and extracellular wall content.

Keywords

Intracranial aneurysms; Animal model; Histological Subtypes

INTRODUCTION

The elastase-induced rabbit aneurysm has been widely used to test new generations of devices[1–7] and to study the hemodynamic milieu of saccular aneurysms.[8–12] Previous studies[12–14] showed that this model has geometry similar to human cerebral aneurysms and has tissue response similar to humans, following platinum coil embolization.[13] However, few previous reports have directly compared rabbit and human histologic factors.

Multiple previous studies have detailed histopathologic findings in human aneurysms, many focused on correlating these findings with rupture status. Frösen, et al[15] analyzed and characterized the cellular milieu in 66 human saccular cerebral aneurysms. Using a 4-point categorical scale, they showed that certain types of histologic findings in human aneurysms were associated with rupture status. In the present study, we retrospectively analyzed the detailed histopathologic evaluations in 27 elastase-induced aneurysms in rabbits and compared these findings with human cerebral aneurysms as detailed by Frösen et al[1516] We aimed to determine whether rabbit histologic characteristics recapitulate the full range of the findings in humans.

MATERIALS AND METHODS

Aneurysm Samples

Twenty-seven elastase-induced female rabbit aneurysms were used for the present retrospective study. The aneurysm creation procedure has been described previously.[18] All animal procedures were approved by the Institutional Animal Care and Use Committee at our organization. After the animals were euthanized, aneurysm samples were harvested at 2 weeks (n=5) and 12 weeks (n=22). The 27 harvested samples were fixed in 10% neutral buffered formalin and underwent regular tissue processing, embedded in paraffin. The paraffin blocks were sectioned at 4 μm in a coronal orientation, permitting long-axis sectioning of the aneurysm dome, neck, and parent arteries.

Histologic Analysis and Immunohistochemistry

For standard histologic evaluation, the sections were stained with hematoxylin-eosin (H&E) and Verhoeff van Gieson. For immunohistochemistry, sections were prepared as previously described.[19] Briefly, sections were pretreated with 0.1 mol/L citric acid buffer and microwaved for 15 minutes. They were incubated in hydrogen peroxide (0.3% in distilled water; 20 minutes), followed by incubation with normal 5% horse serum (20 minutes; 37°C), and then with primary antibody (SMA, Dako; CD31, Dako) at 37°C for 1 hour. Next, they were incubated with primary antibody at 4°C overnight. Slides were rinsed in

phosphate-buffered saline (PBS) and incubated with biotinylated secondary horse antimouse immunoglobulin G (Vector Laboratories). Sections were rinsed in PBS and incubated with Vectastain Elite ABC Reagent (Vector Laboratories) for 45 minutes at 37°C. Finally, slides were developed with diaminobenzidine-tetrahydrochloride (Vector Laboratories). Negative controls were performed with nonimmune, normal serum versus the primary antibody.

Histologic Subtyping

Two trained pathologists (S.W. and D.D.) with more than 10 years' experience interpreted the stained sections and classified the aneurysm wall structure. This wall was compared with human aneurysm wall and the classification reported by Frösen et al[15,16] We segregated the investigated aneurysmal wall into 3 regions: neck area at and near interface between parent artery and aneurysm wall; proximal wall, defined as the wall along the aneurysm's proximal aspect; and distal wall, defined as the wall along the aneurysm's distal aspect. Scoring was performed using a semiquantitative scale and 4 distinct subtypes based on cellular and extracellular matrix findings. Subtypes were A, endothelialized wall with linearly organized SMC; B, thickened wall with disorganized SMC; C, thick, collagenized and hypocellular wall with or without organizing thrombosis and D, extremely thin, hypocellular wall. A single aneurysm region (neck and proximal and distal walls) may manifest multiple subtypes.

RESULTS

Conventional Histopathologic and Immunohistochemistry Findings

At the 2-week point, the elastic lamina was completely or almost completely degraded within the aneurysmal cavity walls. Distribution of endothelial cells was variable across the sac. In some regions, endothelial coverage was discontinuous or completely absent, whereas other areas appeared normal. A thickened wall with proliferating smooth muscle–like cells or neointima hyperplasia was observed in large regions of the wall for all aneurysms at this time point. Neointima hyperplasia was found primarily at the transition zone from the parent artery to the proximal part of the aneurysm wall. While some regions were hypocellular, the wall was not thin. Acute inflammatory cell infiltration was observed in 1 of 5 aneurysms; inflammatory cells were absent in the other 4 aneurysms.

At 12 weeks, the elastic lamina was completely degraded in all specimens. Although the neck region still appeared thickened with a proliferation of smooth muscle like cells, the remainder of the sac was largely replaced with collagenized tissue, devoid of cellular elements. SMA-positive cells were barely detected. No inflammatory infiltrate was found within the aneurysmal walls at this time point. A laminated, organized thrombus was found at the apices of the aneurysm dome in 2 of the 23 samples.

Histologic Subtypes

Findings compatible with all 4 subtypes of human aneurysm tissue were identified (Figure 1). Overall, types A and C were found in 13 (48%) and 11 (41%) of 27 aneurysms and were present in the proximal and distal walls at both time points (Figure 2). Type B was found in

16 aneurysms (59%), exclusively at the neck at both time points. Type D was found in 14 aneurysms (52%), exclusively at the proximal and distal walls of 12-week subjects.

In Figure 3, distribution of wall types within the neck and sac is considered for the time points. By 2 weeks, the neck was solely type B and was unchanged at 12 weeks. In contrast, the sac is heterogeneous at both time points and displays a shifting wall type from more than 80% of types A and B at 2 weeks to more than 70% of types C and D at 12 weeks.

DISCUSSION

This study demonstrates that categories of histologic change seen in human aneurysm tissue are mimicked in the elastase-induced aneurysm model in rabbits. Each of the 4 primary categories described by Frösen, et al[15,16] was observed in the rabbit samples. We noted substantial variation in subtypes not only on the basis of location within the aneurysm cavity but also over time. Types A, B, and C were present at both time points. These 3 types are associated with relatively lower rates of rupture at presentation than type D in clinical specimens. The neck region exclusively had type B, characterized by neointima hyperplasia. Of note, type D—universally associated with rupture in clinical specimens—was seen in the vast majority of rabbit samples at 12 weeks but was absent in the 2-week samples.

Lack of an intact elastic lamina is a common finding for human cerebral aneurysms.[15,20–22] Consistent with these results, the rabbit model shows disruption or some loss of elastic lamina at 2 weeks and complete loss at 12 weeks. Loss of endothelium, reported in 50% of human intracranial aneurysms[15] and believed to be important in aneurysm wall degeneration, [15] was found in the rabbit wall types.

Although wall heterogeneity was not the focus of their work, Frösen et al[15] noted that several aneurysm walls showed gradual change from type A or B to type C or D, mostly in the direction of neck to fundus. Obtaining entire human aneurysm sacs for analysis is difficult, yet Tulamo et al[17] reported 1 case where they found a progressive change from type B (neck) to type C to type D. These findings are consistent with our 12 results that showed progression of type B at the neck to largely types C and D in the proximal and distal walls.

Previous studies have noted histologic changes in the rabbit elastase-induced model.[23,24] Compatible with our current findings, the prior studies noted thin, hypocellular aneurysm walls. The present study extends those studies by using a categorical scale based on human aneurysm specimens categories shown to correlate with proportion of ruptured versus unruptured status at presentation.[15]

The rabbit model offers some advantages over clinical tissue. The entire aneurysm cavity can be evaluated in rabbits whereas human tissue, when excised during aneurysm surgery, usually consists of small segments of the aneurysm dome. Further, the rabbit model can be used to explore progression of the aneurysm wall at multiple time points. Frösen et al[15] conjectured that the histologic wall types identified for humans reflect progressive wall degeneration. This conjecture, which cannot be studied directly in human patients, is supported by the changes seen in the rabbit model. Herein, we describe a progressive shift

from a wall dominated by types A and B at 2 weeks to predominantly types C and D at 12 weeks. Progressive changes in the aneurysm wall is the focus of ongoing investigation using the rabbit model.[25] Together, these findings suggest that the rabbit model might offer utility in testing systemic or local therapies aimed at modulating histologic progression to subtypes associated with rupture.

The pathophysiology of human intracranial aneurysms is complex and it is related to genetic background; previous disease history such as hypertension, cholesterol deposit, wall inflammation and life style such as smoking.[26–28] On the contrary, the elastase induced rabbit model reported in the current study does not have those mentioned above, which is the limitation to all the animal models including the elastase induced rabbit model described in the current study; however, our previous studies demonstrated that, the elastase-induced saccular aneurysm in rabbit, is similar to human intracranial saccular aneurysms geometrically and hemodynamically, which included: 1) location along a curved vessel with anatomy that simulates human aneurysms such as those in the ophthalmic region;[14] 2) aneurysm size similar to the mean size of human cerebral aneurysms;[29] 3) long term patency;[30] 4) shares some molecular features with human intracranial aneurysms;[31] 5) hemodynamic and geometric features are qualitatively and quantitatively similar to those seen in large numbers of human cerebral aneurysms.[12] In addition, the healing process in the rabbit model after embolization with platinum coils mimics the healing seen in human aneurysms.[13] Because the aneurysm model does not undergo spontaneous rupture, we are limited to analyses of changes over time rather than correlating findings to rupture risk. Further, lack of full knowledge of the location of human aneurysm tissue relative to the aneurysm neck versus dome limits direct comparison between the 2 species. Organizing thrombus was reported in the lumen of 21% of unruptured and 60% of ruptured aneurysms.[15] However, it was identified only in the dome of some of the rabbit aneurysms. Finally, because the apex of the rabbit aneurysm dome consists of organizing thrombus, based on the mode of construction with distal ligation, we are unable to evaluate histologic changes high in the aneurysm cavity.

CONCLUSIONS

The wall of the elastase-induced rabbit aneurysm model reproduces the histologic categories found in human aneurysms and offers an opportunity for studying progressive changes in the aneurysm wall.

Acknowledgments

FUNDING STATEMENT

This study was supported by funds from the National Institutes of Health under grants R01NS076491, R01NS042646 and R21NS088256. The content is solely the responsibility of the authors and does not necessarily represent the official views of the National Institutes of Health.

References

1. Dai D, Ding YH, Danielson MA, et al. Endovascular treatment of experimental aneurysms with use of fibroblast transfected with replication-deficient adenovirus containing bone morphogenetic

protein-13 gene. AJNR American journal of neuroradiology. 2008; 29(4):739–44. [published Online First: 2008/01/11]. DOI: 10.3174/ajnr.A0892 [PubMed: 18184848]

2. de Gast AN, Altes TA, Marx WF, et al. Transforming growth factor beta-coated platinum coils for endovascular treatment of aneurysms: an animal study. Neurosurgery. 2001; 49(3):690–4. [published Online First: 2001/08/29]. [PubMed: 11523681]
3. Ding YH, Dai D, Lewis DA, et al. Angiographic and histologic analysis of experimental aneurysms embolized with platinum coils, Matrix, and HydroCoil. AJNR American journal of neuroradiology. 2005; 26(7):1757–63. [published Online First: 2005/08/11]. [PubMed: 16091526]
4. Kallmes DF, Ding YH, Dai D, et al. A new endoluminal, flow-disrupting device for treatment of saccular aneurysms. Stroke; a journal of cerebral circulation. 2007; 38(8):2346–52. STROKEAHA. 106.479576 [pii] [published Online First: 2007/07/07]. DOI: 10.1161/STROKEAHA.106.479576
5. Kallmes DF, Ding YH, Dai D, et al. A Second-Generation, Endoluminal, Flow-Disrupting Device for Treatment of Saccular Aneurysms. American Journal of Neuroradiology. 2009; 30(6):1153–58. DOI: 10.3174/ajnr.A1530 [PubMed: 19369609]
6. Kallmes DF, Fujiwara NH, Yuen D, et al. A collagen-based coil for embolization of saccular aneurysms in a New Zealand White rabbit model. AJNR American journal of neuroradiology. 2003; 24(4):591–6. [published Online First: 2003/04/16]. [PubMed: 12695186]
7. Killer M, Kallmes DF, McCoy MR, et al. Angiographic and histologic comparison of experimental aneurysms embolized with hydrogel filaments. AJNR American journal of neuroradiology. 2009; 30(8):1488–95. [published Online First: 2009/05/29]. DOI: 10.3174/ajnr.A1649 [PubMed: 19474120]
8. Kadirvel R, Ding YH, Dai D, et al. The influence of hemodynamic forces on biomarkers in the walls of elastase-induced aneurysms in rabbits. Neuroradiology. 2007; 49(12):1041–53. [published Online First: 2007/09/21]. DOI: 10.1007/s00234-007-0295-0 [PubMed: 17882410]
9. Zeng Z, Durka MJ, Kallmes DF, et al. Can aspect ratio be used to categorize intra-aneurysmal hemodynamics?--A study of elastase induced aneurysms in rabbit. Journal of biomechanics. 2011; 44(16):2809–16. [published Online First: 2011/09/20]. DOI: 10.1016/j.jbiomech.2011.08.002 [PubMed: 21925661]
10. Zeng, Z., Kallmes, DF., Ding, Y., et al. Hemodynamics of elastase induced aneurysms in rabbut- A new high flow bifurcation model. Proceedings od the ASME 2011 Summer Bioengineering Conference; 2011; p. SBC2011-53819.
11. Zeng Z, Kallmes DF, Durka MJ, et al. Sensitivity of CFD based hemodynamic results in rabbit aneurysm models to idealizations in surrounding vasculature. Journal of biomechanical engineering. 2010; 132(9):091009. [published Online First: 2010/09/08]. doi: 10.1115/1.4001311 [PubMed: 20815643]
12. Zeng Z, Kallmes DF, Durka MJ, et al. Hemodynamics and anatomy of elastase-induced rabbit aneurysm models: similarity to human cerebral aneurysms? AJNR American journal of neuroradiology. 2011; 32(3):595–601. [published Online First: 2011/01/29]. DOI: 10.3174/ajnr.A2324 [PubMed: 21273353]
13. Dai D, Ding YH, Danielson MA, et al. Histopathologic and immunohistochemical comparison of human, rabbit, and swine aneurysms embolized with platinum coils. AJNR American journal of neuroradiology. 2005; 26(10):2560–8. [published Online First: 2005/11/16]. [PubMed: 16286401]
14. Short JG, Fujiwara NH, Marx WF, et al. Elastase-Induced Saccular Aneurysms in Rabbits: Comparison of Geometric Features with Those of Human Aneurysms. American Journal of Neuroradiology. 2001; 22(10):1833–37. [PubMed: 11733310]
15. Frösen J, Piippo A, Paetau A, et al. Remodeling of Saccular Cerebral Artery Aneurysm Wall Is Associated With Rupture. Histological Analysis of 24 Unruptured and 42 Ruptured Cases. 2004; 35(10):2287–93. DOI: 10.1161/01.STR.0000140636.30204.da
16. Frosen J, Piippo A, Paetau A, et al. Growth factor receptor expression and remodeling of saccular cerebral artery aneurysm walls: implications for biological therapy preventing rupture. Neurosurgery. 2006; 58(3):534–41. discussion 34–41. DOI: 10.1227/01.NEU.0000197332.55054.C8 [PubMed: 16528195]

17. Tulamo R, Frösen J, Hernesniemi J, et al. Inflammatory changes in the aneurysm wall: a review. Journal of NeuroInterventional Surgery. 2010; 2(2):120–30. DOI: 10.1136/jnis.2009.002055 [PubMed: 21990591]
18. Altes TA, Cloft HJ, Short JG, et al. 1999 ARRS Executive Council Award. Creation of saccular aneurysms in the rabbit: a model suitable for testing endovascular devices. American Roentgen Ray Society. AJR American journal of roentgenology. 2000; 174(2):349–54. [published Online First: 2000/02/05]. [PubMed: 10658703]
19. Dai D, Ding YH, Danielson MA, et al. Modified histologic technique for processing metallic coil-bearing tissue. AJNR Am J Neuroradiol. 2005; 26(8):1932–6. [PubMed: 16155137]
20. Scott S, Ferguson GG, Roach MR. Comparison of the elastic properties of human intracranial arteries and aneurysms. Canadian journal of physiology and pharmacology. 1972; 50(4):328–32. [published Online First: 1972/04/01]. [PubMed: 5038350]
21. Tada Y, Austin G1FS, Dickson D, Anderson D, Richardson S. he significance of the extracellular matrix in intracranial aneurysms. Ann Clin Lab Sci. 1993; 23(2)
22. Robertson AM, Watton PN. Computational Fluid Dynamics in Aneurysm Research: Critical Reflections, Future Directions. American Journal of Neuroradiology. 2012; 33(6):992–95. DOI: 10.3174/ajnr.A3192 [PubMed: 22653325]
23. Bouzeghrane F, Naggara O, Kallmes DF, et al. In vivo experimental intracranial aneurysm models: a systematic review. AJNR American journal of neuroradiology. 2010; 31(3):418–23. ajnr.A1853 [pii] [published Online First: 2009/10/31]. DOI: 10.3174/ajnr.A1853 [PubMed: 19875466]
24. Cesar L, Miskolczi L, Lieber BB, et al. Neurological deficits associated with the elastase-induced aneurysm model in rabbits. Neurological research. 2009; 31(4):414–9. ner1521 [pii] [published Online First: 2008/10/02]. DOI: 10.1179/174313208X346918 [PubMed: 18826754]
25. Sang, C., Kallmes, DF., Kadirvel, R., et al. Mechanical Response and Fiber Remodeling in Elastase-Induced Rabbit Aneurysms. 5th International Conference on Computational and Mathematical Biomedical Engineering – CMBE2017; 2017. p. 1300-03.
26. Fan J, Sun W, Lin M, et al. Genetic association study identifies a functional CNV in the WWOX gene contributes to the risk of intracranial aneurysms. Oncotarget. 2016; 7(13):16104–11. DOI: 10.18632/oncotarget.7546 [PubMed: 26910372]
27. Keedy A. An overview of intracranial aneurysms. Mcgill J Med. 2006; 9(2):141–6.
28. Qureshi AI, Suarez JI, Parekh PD, et al. Risk factors for multiple intracranial aneurysms. Neurosurgery. 1998; 43(1):22–6. discussion 26–7. [PubMed: 9657184]
29. Short JG, Fujiwara NH, Marx WF, et al. Elastase-induced saccular aneurysms in rabbits: comparison of geometric features with those of human aneurysms. AJNR Am J Neuroradiol. 2001; 22(10):1833–7. [PubMed: 11733310]
30. Ding YH, Dai D, Lewis DA, et al. Long-term patency of elastase-induced aneurysm model in rabbits. AJNR Am J Neuroradiol. 2006; 27(1):139–41. [PubMed: 16418373]
31. Mangrum WI, Farassati F, Kadirvel R, et al. mRNA expression in rabbit experimental aneurysms: a study using gene chip microarrays. AJNR Am J Neuroradiol. 2007; 28(5):864–9. [PubMed: 17494658]

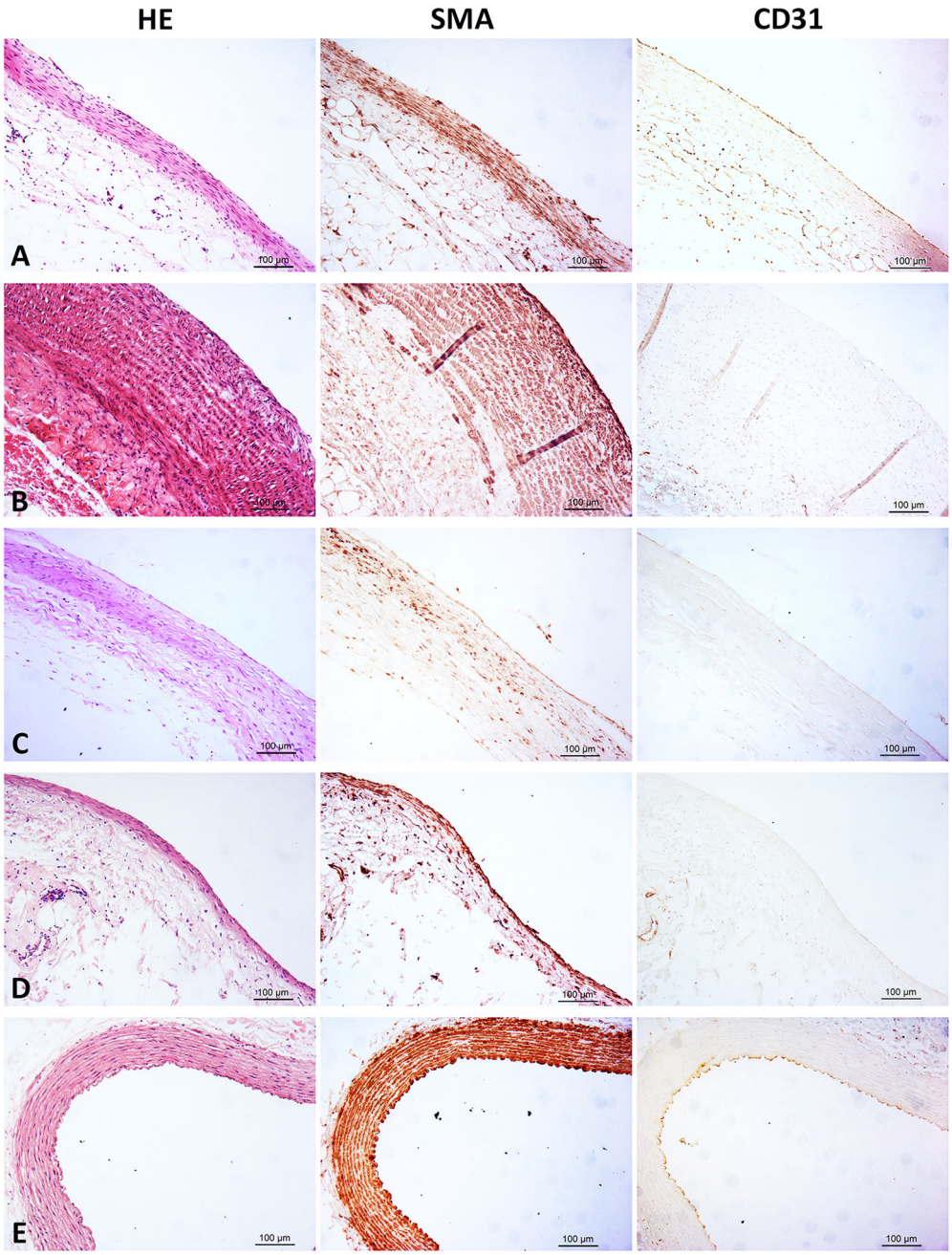

Figure 1.

Representative Images of the 4 Subtypes of Human Intracranial Aneurysms Identified in the Rabbit Model (From left to right, first column is Hematoxylin &eosin (H&E), middle column is immunohistochemistry(IHC) for α-smooth muscle action (SMA) and the right column is IHC for CD31; original magnification 200× for all photos). A (Type A), Linear organized SMC and intact endothelium, the lumen side of the wall is still lined with CD31 + cells. B (Type B), Thickened wall with disorganized, prolifering SMC postivie cells; the wall lacks CD31 positive cells coverage. C (Type C), Thick, collagenized, hypocelluar wall with/ without CD31 positive cells coverage. D (Type D), Extremely thin and decellularized wall.

E, Normal right common carotid artery wall of rabbit. The media of the wall is composed of 11–12 layers of well-organized SMA positive cells, and it is lined with intact CD31 positive cells.

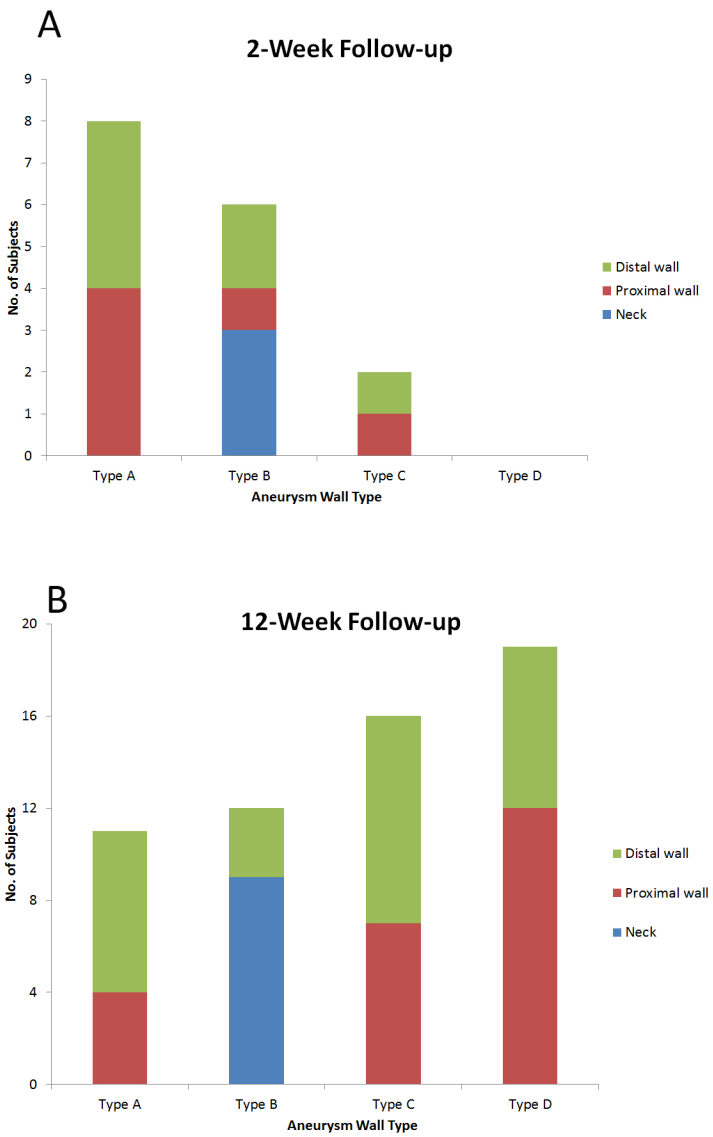

Figure 2.

Rabbit Aneurysm Sacs That Display Each Human Aneurysm Wall Subtype by Sac Region. A, At 2-Week Follow-up. B, At 12-Week Follow-up.

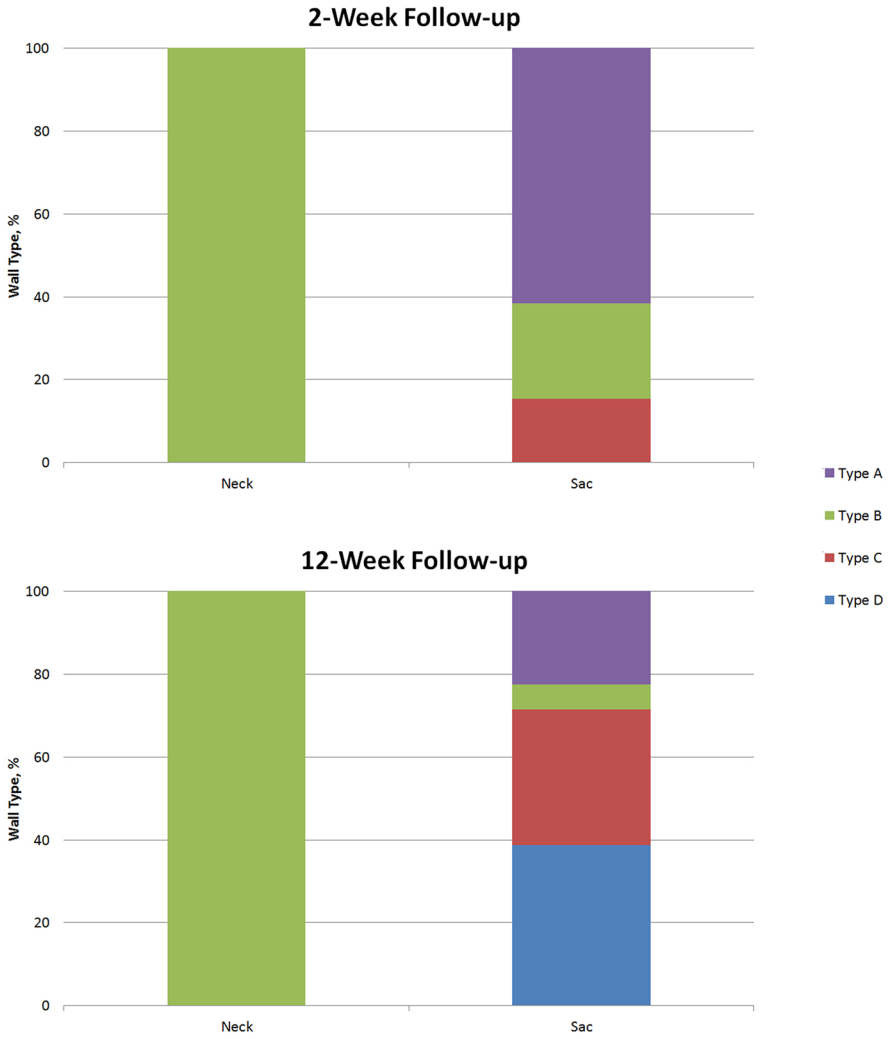

Figure 3.
Percentages of Aneurysm Wall Subtypes at 2- and 12-Week Follow-up by Neck and Sac Region.